ARTICLE

Check for updates

Exposure to oxybenzone from sunscreens: daily transdermal uptake estimation

Azin Eftekhari[1] ✉ and Glenn C. Morrison[1]

BACKGROUND: Fugacity, the driving force for transdermal uptake of chemicals, can be difficult to predict based only on the composition of complex, non-ideal mixtures such as personal care products.
OBJECTIVE: Compare the predicted transdermal uptake of benzophenone-3 (BP-3) from sunscreen lotions, based on direct measurements of BP-3 fugacity in those products, to results of human subject experiments.
METHODS: We measured fugacity relative to pure BP-3, for commercial sunscreens and laboratory mixtures, using a previously developed/solid-phase microextraction (SPME) method. The measured fugacity was combined with a transdermal uptake model to simulate urinary excretion rates of BP-3 resulting from sunscreen use. The model simulations were based on the reported conditions of four previously published human subject studies, accounting for area applied, time applied, showering and other factors.
RESULTS: The fugacities of commercial lotions containing 3–6% w/w BP-3 were ~20% of the supercooled liquid vapor pressure. Simulated dermal uptake, based on these fugacities, are within a factor of 3 of the mean results reported from two human-subject studies. However, the model significantly underpredicts total excreted mass from two other human-subject studies. This discrepancy may be due to limitations in model inputs, such as fugacity of BP-3 in lotions used in those studies.
SIGNIFICANCE: The results suggest that combining measured fugacity with such a model may provide order-of-magnitude accurate predictions of transdermal uptake of BP-3 from daily application of sunscreen products.

Keywords: Dermal uptake; Skin; Chemical activity; Fugacity; Exposure model; Personal care products

Journal of Exposure Science & Environmental Epidemiology; https://doi.org/10.1038/s41370-021-00383-9

INTRODUCTION

Sunscreens have been widely recommended because of increasing incidences of different types of skin cancer [1–5]. The rise in sunscreen use has led to concerns about health effects of some sunscreen ingredients [6]. Although there is no question that sunscreens are protective against harmful ultraviolet radiation from the sun [7–9], there has been an increased concern regarding transdermal uptake of some active ingredients (also known as ultraviolet light inhibitors, or UV inhibitors) of sunscreens which are suspected to be endocrine disrupting chemicals [10–16].

One of the UV inhibitors of concern is a phenolic compound commonly called benzophenone-3 (BP-3) or oxybenzone (2-hydroxy-4-methoxybenzophenone). BP-3 is a highly lipophilic organic compound which absorbs and dissipates both long wave ultraviolet-A and short wave ultraviolet-B [17]. BP-3 is among the most commonly used ultraviolet light absorbing components in medicine, cosmetics, skin, and hair products. Health concerns arose when in vivo and in vitro animal studies showed associations between BP-3 exposure and levels of sex hormones such as estrogen and testosterone [6, 18–25]. It has been shown in rats and humans that BP-3 can be metabolized to metabolites such as 2,4-dihydroxybenzophenone or benzophenone-1 (BP-1) and 2,2′,4,4′-tetrahydroxybenzophenone or benzophenone-2 (BP-2) [26–28]. In vitro studies have shown that BP-1, the major metabolite of BP-3, has even stronger estrogenic activity than BP-3. Antiandrogenic activity of BP-1 has been also observed in vitro studies [29]. Epidemiologic studies have shown an association between BP-3 (and its metabolites) and endometriosis [30], shorter pregnancy time, and possible decrease in fetal growth [25, 31–33]. Based on current regulations in the USA, BP-3 can be present at up to 6 weight percent (% w/w) of sunscreen products and 0.5% w/w of other personal care products [34]. It can also be found in infant clothing and pantyhose [35, 36]. The European Union reduced the maximum allowable level of BP-3 in sunscreens from 10% to 6% w/w, after February 2017 [37].

Due to BP-3 health concerns, potential dermal exposure of humans to these hormone disruptive chemicals is important in the safety assessment of commercially available personal care products. Several in vivo and in vitro animal and human studies have shown that substantial amounts of BP-3 can be absorbed through the skin from sunscreen lotions [10, 11, 13–16, 38, 39]. In addition to in vivo and in vitro studies, simulation models have been developed to help quantify risks associated with transdermal uptake of chemicals of concern.

[1]Department of Environmental Sciences and Engineering, Gillings School of Global Public Health, The University of North Carolina at Chapel Hill, Chapel Hill, NC, USA. ✉email: azinef@ad.unc.edu

Received: 6 March 2021 Revised: 19 August 2021 Accepted: 20 August 2021
Published online: 16 September 2021

In our recent publication [40], we discussed the importance of fugacity of compounds of mixtures, in particular in non-ideal solutions, in exposure studies and toxicokinetic models [41–46]. Here, fugacity is assumed to be identical to the equilibrium partial pressure of a compound in the gas-phase over the mixture. We measured fugacity of two phathalates and a paraben in cosmetic cream (relative to pure compounds, relative fugacity or $\acute{F}_{BP-3}$) using a solid-phase microextraction (SPME) method. We showed that the relationship between the fugacities and chemical concentrations is non-linear and used these results in a mass transfer model to predict transdermal uptake of the target chemicals. The non-linear relationship between fugacity and concentration in these non-ideal complex mixtures suggested that linear extrapolation from in vivo data at one concentration should not be used to predict uptake at other concentrations. Instead, fugacity measured at the appropriate mixture concentration is better for use in transdermal uptake models.

Since only a limited number of in vivo controlled experimental studies are available to test the model, we aim to test our model by simulating transdermal uptake scenarios based on four different human subject experiments (from 1997 to 2006) where they studied uptake of BP-3 from sunscreen lotions. Therefore, specific objectives are to (1) use the measured fugacity to predict transdermal uptake of BP-3 using Eftekhari et al. [40]. model for four scenarios based on human subject experiments by Hayden [13] Gonzalez et al. [15]. Sarveiya et al. [38], and Gonzalez et al. [39] and (2) compare model predictions to human subject results to assess model performance. To address questions raised in Eftekhari et al. [40], additional objectives are to (3) measure fugacity of BP-3 in lab-made and commercial sunscreen lotions and their dilutions and assess the relationship between fugacity and concentration, (4) test the hypothesis that the low-volatility, oily, components of sunscreen influence the resulting fugacity more than watery components, (5) compare in vitro measurements of fugacity with that for the mixture after it has been applied to skin.

MATERIALS AND METHODS

Materials

WELLSKIN Glaxal Base was purchased through Amazon. Lotion ingredients as reported on its label are water, petrolatum, cetearyl alcohol, paraffinum liquidum, cereareth-20, sodium phosphate and p-chloro-m-cresol. Benzophenone-3 (BP-3), octyl-methoxycinnamate (OMC) and 3-(4-methylbenzylidene) camphor (4-MBC) were purchased from Sigma-Aldrich. Commercially available sunscreens were purchased from a retail store in Chapel Hill (NC, USA): Coppertone Sport Clear Lotion Sunscreen SPF 50, Coppertone Ultraguard Lotion Sunscreen SPF 70, Coppertone Sport Spray Suncreen SPF 50, Hawaiian Tropic Sheer Touch Lotion Sunscreen SPF 15, Hawaiian Tropic Island Sport Lotion Sunscreen SPF 50, Neutrogena Clear Face Lotion Sunscreen SPF 55, Neutrogena Age Shield Face Lotion Sunscreen SPF 70, Neutroena Ultra Sheer Sunscreen Stick SPF 70, and Trader Joe's Spray Sunscreen SPF 50. Section 1 and Table S1 of the Supporting Information (SI) lists the commerical sunscreens, their brands, and active ingredients.

Methods

Commercial and lab-made sunscreen products. Two different stock formulations of lab-made sunscreen mixtures were prepared as follows: 10% (w/w) BP-3 in Glaxal Base cream, and 10% each of BP-3, OMC and 4-MBC combined in Glaxal Base. The second mixture includes two additional UV inhibitors that have commonly been used in sunscreen formulations. The mixtures were stirred for 2 min, 3–5 times a day for 1 week, using a glass rod. Sonicator and vortex mixer were also used in between manual stirring until the mixure appeared (visually) to be uniform and well-mixed before preparing dilutions. The homogeneity of the solutions was checked by headspace solid phase micro-extraction (SPME) GC-FID analysis of three small portions of each solution. The mixture was considered well-mixed if the signal was the same across these three samples. Each of the two stock solutions were sequentially diluted by a factor of three, resulting in concentrations that ranged between 0.123% to 10%. Coppertone brand sunscreen lotions with 6% and 0% BP-3 and Hawaiian brand sunscreen lotions with 4% and 0% BP-3 were also chosen for preparing dilutions from commercial sunscreen products. Each BP-3-containing sunscreen and the same-brand sunscreen without BP-3 were mixed using the aforementioned mixing protocol to prepare dilutions in the range of 0.1–4% for Hawaiian sunscreen and 0.5–6% for Coppertone sunscreen. About 0.5 g of each commercial sunscreen, dilutions of commercial sunscreens and dilutions of BP-3 in Glaxal Base cream were added to 20 ml glass SPME vials (triplicate of each concentration). The mixture was spread over the entire inner surface of the vial. A vial of pure Glaxal Base lotion was prepared as a laboratory blank. Commercial sunscreens containing no BP-3 were also designated as commercial lotion "blank" samples. A vial of pure BP-3 was prepared as a SPME/GC-FID reference, specifically a fugacity reference. About 0.5 g of BP-3 powder was transferred to a SPME vial, the vial inner walls were warmed to melt BP-3and the vial was tilted and rotated so that the walls were coated with melted BP-3. It was then allowed to cool so that a thin layer of solid BP-3 formed on the vial walls.Water content of lotions

We examined the hypothesis that the low-volatile, oily, components of sunscreen strongly influence the resulting fugacity of BP-3. Conversely, the more volatile components (assumed to be primarily water), only weakly influence the fugacity of BP-3 in the mixture. The volatile fractions of Glaxal base cream and commercial sunscreen lotions were determined as follows. Approximately 1 g of each lotion was spread in a thin layer on the bottom of an aluminum weighing boat. The mass of fresh lotions were recorded and the aluminum weighing boats were placed in an oven at 60 °C. The mass of oven-treated lotions were recorded after 1, 2, and 24 h placement in the oven. The lotions were allowed to cool to laboratory temperature before weighing. The measurement showed that 2 h was a sufficient oven-treatment time for all lotions, i.e., the mass did not change after 2 h. The mass of dry lotions based on 2-h drying time was used for water content analysis (assuming that most of the volatile mass is comprised of water) and for calculating the concentration of BP-3 in the non-volatile component of the lotions.

Relative fugacity ($\acute{F}_{BP-3}$) measurement. A gas chromatograph with a flame ionization detector equipped with a SPME inlet (SPME/GC-FID) was used for headspace sample analysis (see SI, Section 2 for GC-FID method). SPME headspace sampling of the vials of commericial sunscreens, mixtures of BP-3 in Glaxal, dilutions of commercial suscreens, blank, and pure solid BP-3 as SPME reference was carried out at 32 °C using a 7 µm PDMS SPME fiber (fused silica, 23 Ga, green). After testing different SPME headspace sampling times that ranged from 7 to 60 min, a method was developed using a 14 min extraction time. For BP-3 and this SPME fiber, this time lies within the linear, kinetically limited absorption range (see SI Section 3, Eftekhari et al. [40]. and Fig. S1).

Pure solid BP-3 in a SPME vial was used as the fugacity reference and as an internal standard for SPME analysis. The measured relative fugacity of BP-3, $\acute{F}_{BP-3}$, is defined as the GC-FID peak area for the sunscreen cream headspace sample, $FID_{cream,BP-3}$, divided by the headspace peak area for the pure compound, $FID_{pure,BP-3}$, after correcting for the sub-cooled liquid vapor pressure. The need for this correction is due to the fact that BP-3 used as the fugacity reference in our measurement is a solid at 32 °C (skin temperature). The ratio of sub-cooled liquid and solid phase vapor pressures, $P_{v,BP-3,liquid}$ and $P_{v,BP-3,solid}$ is used to calculate the corrected $\acute{F}_{BP-3}$:

$$\acute{F}_{BP-3} = \left(\frac{FID_{cream,BP-3}}{FID_{pure,BP-3}}\right)\left(\frac{P_{v,BP-3,solid}}{P_{v,BP-3,liquid}}\right) \quad (1)$$

where,

$$\frac{P_{v,BP-3,solid}}{P_{v,BP-3,liquid}} = -\frac{\Delta H_{fus,BP-3}}{RT_{mp,BP-3}}\left(1 - \frac{T_{mp,BP-3}}{T}\right) \quad (2)$$

R is the gas constant (8.314 J/mol K), $\Delta H_{fus,\,BP-3}$ is the enthalpy of fusion (21.77 kJ/mol), and $T_{mp,\,BP-3}$ is the melting point temperature (336.7 K). The solid/liquid vapor pressure correction factor of 0.447 was calculated using the experimentally measured enthalpy of fusion reported by Lago et al. [47]. (See Section 4 of SI for the details of an experiment used confirm the use of the sub-cooled liquid vapor presuure to correct the relative fugacity). The near-lotion gas phase concentration of BP-3 is calculated using Eq. (3) for use as input for the transdermal uptake model:

$$C_{g,BP-3} = \frac{\acute{F}_{BP-3}P_{v,BP-3,liquid}MW_{BP-3}}{RT} \quad (3)$$

where, $\acute{F}_{BP-3}$ ($\frac{g}{mol}$) is BP-3 molecular weight, R ($\frac{m^3 Pa}{Kmol}$) is the ideal gas constant, and T (K) is skin temperature (assumed 32 °C or 305.15 K).

We also measured the $\acute{F}_{BP-3}$ of commercial sunscreens on the fore-arm skin of one of the coauthors. Washable skin markers were used to mark a 2 cm^2 skin area on the arm. An average of 20 mg of a brand sunscreen lotion was applied within the square indicated by the marked corners. Lotion was allowed to remain on skin to dry for at least for 20 min before the first skin SPME headspace sampling. Fisherbrand weighing funnels made of borosilicate glass (stem diameter: 10.25 mm OD and 8.12 mm ID, top diameter: 25 mm) were used for skin SPME headspace sampling (we call it SPME headspace skin sampler hereafter). The funnel is placed upside down over the skin to create an enclosed volume over the skin. The SPME headspace skin sampler was taped on top of the lotion on the arm. Fisher brand turnover septum stoppers were used at the end of weighing funnel stem to hold the SPME fiber in place during skin headspace sampling (see SI, Fig. S2 for the picture of SPME headspace skin sampler). A 20 min extraction time was chosen after testing different extraction time for SPME headspace skin sampling (see SI, Fig. S3). This method of headspace skin sampling was inspired by Duffy et al. [48]. After each brand sunscreen was applied to the skin, SPME headspace skin sampling was repeated to monitor any changes in the $\acute{F}_{BP-3}$ of BP-3 over time. To measure a "skin-free" reference fugacity using the SPME headspace skin sampling method, we applied pure BP-3 on a piece of an aluminum foil which was then placed on the arm (and therefore close to skin temperature) and secured with a piece of tape. The SPME headspace skin sampler was then placed on the foil and sampled as described above.

SIMULATION OF TRANSDERMAL UPTAKE FROM LOTION

Model framework and parameters

In this study, we test the Eftekhari et al. model [40] using the results of four human subject studies (see Section 3.2). In these experiments, resarchers applied sunscreens containing BP-3 on the skin of volunteers and collected urine. In our model, we assumed skin lipids are effectively "replaced" by the lotion (when lotion is present) and the calculated lotion thickness was used in the model instead of skin lipid thickness. After each shower, the lotion layer is replaced with skin lipids and BP-3 concentration of the skin surface lipids are set to zero until the next time-step of the simulation. Although the skin surface lipid layer concentration is set to zero, the BP-3 concentration in the adjacent SC layer is not equal to zero. At the next time step, the SSL accumulates chemicals from the SC to achieve equilibrium and also equilibrates with the overlying air. The model uses the near-lotion BP-3 gas-phase concentration of sunscreens measured in this research as the input for trandermal uptake model. The initial near-lotion gas concentration (μg/m^3) of BP-3 in the model is obtained by multiplying the sub-cooled BP-3 vapor pressure (0.0021 Pa) at 32 °C by the average $\acute{F}_{BP-3}$ of BP-3 from sunscreen lotions at 32 °C (Eqs. 1, 2, and 3). The sub-cooled BP-3 vapor pressure of 0.0021 Pa (Table 1) at 32 °C was interpolated from existing experimental data [47, 49].

The model simulates dynamic Fickian diffusion of BP-3 into distinct skin layers of skin lipids, stratum corneum, and viable epidermis (See SI, Section 5 for the detailed description of the model). Using this model, BP-3 is assumed to be absorbed, rapidly metabolized, and exreted with each urination. To be able to compare the results of the simulation with experimental studies, we use available experimental toxicokinetic factors (f_{tox}) to convert the simulated mass of BP-3 transferred to blood to urinary mass excreted. Since no human-based toxicokinetic factors have been reported, we specified the baseline f_{tox} to be 0.22 based on the only dermal BP-3 exposure experimental results (on rats) that were reported by Okereke et al. [50]. Toxicokinetic factors for BP-3 based on human subjects are not available, to our knowledge. The corrected excreted mass of BP-3 is then compared with the experimental excreted mass for each human subject experiment.

Table 1 shows the physicochemical properties and base-case transdermal uptake model input parameters of BP-3 at 32 °C. SPARC online calculator was used for phyicochemical properties of BP-3 at 32 °C. The vapor pressure of BP-3 at 32 °C was interpolated from existing experimental data [47, 49]. BP-3 diffusion and partition coefficients were estimated based on available models for a partially hydrated stratum corneum [51–54]. See Fig. S4 for the schematic of transdermal uptake of BP-3 from sunscreen lotion. See SI section 6 and Fig. S5 for the screenshot of the spreadsheet which was prepared for calculation of the transdermal uptake model input parameters (The spreadsheet is available from the authors upon request). Detailed calculation of the model input parameters can be found in Eftekhari et al. [40].

Among the base-case model parameters (Table 1), five variables were considered for further sensitivity analysis to study the effects of these variables (lower and higher values relative to base-case values) on prediction of transdermal uptake of BP-3 from sunscreen product in each human subject scenario. The five variables are relative fugacity ($\acute{F}_{BP-3}$), toxicokinetic factor (f_{tox}), diffusion coefficient of BP-3 in stratum corneum (D_{sc}), gas/stratum corneum partition coefficient of BP-3 ($K_{sc/g}$), and stratum corneum thickness (L_{sc}). Based on the lowest and highest measured $\acute{F}_{BP-3}$ of BP-3 for commercial sunscreen products, two independent simulations were run using $\acute{F}_{BP-3}$ of 0.1 and 0.3. Two f_{tox} of 0.15 and 0.3 were used as low and high values for individual simulations [26, 27]. We also ran independent simulations using three times and one third of D_{sc} and $K_{sc/g}$ based on uncertainties for these parameters [40]. L_{sc} of 15 and 30 μm [55–58] were used as high and low values in independent simulations, for comparison with the base-case L_{sc} of 23 μm. In the main manuscript, we only show the results of varying one of the model input parameters ($K_{sc/g}$). See section 4.2, simulation results, for more details on the predicted excreted masses of BP-3 based on varying the rest of the model variables.

Simulation scenarios

Here, we explain how the model parameters were set to simulate conditions of human subject experiments by Gonzalez et al. [39] Sarveiya et al. [38] Gonzalez et al. [15], and Hayden et al. [13]. Differing among the studies were details such as skin area covered, sunscreen brand (not usually reported), concentration of BP-3, time interval of sunscreen application, number of applications, and total monitoring time after initial application. The experimental conditions of Gonzalez et al. [39]. as an example of the method is described in full. The details of the other human subject experiments can be found in the SI, Section 7. Table 1 presents the parameter values reported by those studies and used as inputs in the model to simulate excretion rates for each human subject experiment.

In the study by Gonzalez et al. [39] 25 volunteers with an average age of 27 were randomly divided into two groups: A and B. A commercially available sunscreen lotion containing 4% BP3 was chosen for the study. Urine samples prior to the lotion application were collected. The sunscreen lotion was applied to the whole body (2 mg/cm^2) in the morning and in the evenings for 5 days (ten times in total). Volunteers were allowed one shower per day before the evening-application. Urine samples were collected for 10 days from the first application. The experimental sequence was the same for both groups except that group B received daily UV irradiation through a Dermalight Ultra A1 in the first 5 days of study. They collected urine throughout the study for a 240 h. An average of 3.7% (1.2–8.7%) of the total amount of BP-3 applied throughout the experiment was excreted in urine samples of each participant. They did not observe any significant difference in the extracted fraction of BP-3 between group A and B. Since there was no observed difference [39], we compare our simulations to the results from their entire population.

In our simulation of the average Gonzalez et al. subject [39], we assume a skin surface area of 2 m^2 and application of 2 mg/cm^2 which results in total lotion mass of 40 g (1600 mg BP-3). We assumed skin lipids mix into the lotion and the lotion thickness of 20 μm (40 g lotion/2 m^2 skin surface area) was used as the skin surface lipid

Table 1. Base-case model input and parameters of the model for each human subject scenario.

Base-case transdermal uptake model parameters of BP-3 at 32 °C for partially hydrated stratum corneum (SC).									
L_{sc} (μm)	**L_{ve} (μm)**	**$K_{ve/w}$[a]**	**$K_{ssl/g}$[a]**	**$K_{sc/g}$[a]**	**$K_{ve/g}$[a]**	**D_{sc} m²/s**	**D_{ve} m²/s**	**h_m m/h**	**H_{cp} atm m³/mol**	**P_v Pa**
23	**100**	**5.9**	**2.45×10^9**	**5.03×10^7**	**4.78×10^6**	**4.96×10^{-15}**	**2.64×10^{-11}**	**25**	**3.09×10^{-8}**	**0.0021**
Parameters of the model for each human subject scenario										
Model input parameters				**Gonzalez et al. [39]**		**Sarveiya et al. [38]**		**Gonzalez et al. [15]**		**Hayden [13]**
Skin surface area (m²)				21.875		0.086		2		0.1051
sunscreen applied (g)				37.5		1.7		40		13
Sunscreen applied (mg/cm²)				1.71		2.0		2.0		12.4
% BP-3 in sunscreen				4		6		4		6
BP-3 applied (mg)				1600		102		1600		780
Lotion thickness (μm)				20		19.8		20		123.7
Days of lotion application				5		1		1		1
Numbers of lotion application/day				2		1		1		1
Time between two applications[b]				12		-		-		-
Numbers of shower/day[c]				1		1		1		1
Time between application and shower				11		8		12		12
Urine collection period (h)				240		48		38		48

[a]Dimensonless, ratio of the equilibrium concentration of BP-3 in phase 1 to the concentration in phase 2 (for example concentration of BP-3 in viable epidermis to the concentration of BP-3 in water, (μg/m³)/(μg/m³)); consistent with recent models, partition coefficients of skin layers are all referenced to the gas-phase concentration [54, 59, 60].
[b]One morning and one evening application. For the model, we assume 12 h between each application.
[c]One shower per day, before the second application.

thickness (L_{ssl}) before showering. In the model, we assume time interval of 12 h between morning and evening applications and the shower happens 1 h before evening application. We assume each shower effectively removes lotion and BP-3 from the skin and L_{ssl} becomes 1.2 µm (typical skin lipid thickness based on literature values [54, 55, 59]) after the shower until the next lotion application. See the Results Section for the chosen base-case $\acute{F}_{BP-3}$ used in the simulation.

To compare the model to the human subject experiments, some results had to be estimated from figures or converted from tabular results in those papers. The daily excreted BP-3 masses were visually estimated from Fig. 2 of Gonzalez et al. [39] and converted to the cumulative excreted BP-3. Gonzalez et al. [15] cumulative excreted BP-3 was visually estimated directly from their Fig. 2. The skin area-normalized cumulative excreted masses of BP-3 by human subjects reported by Sarveiya et al. [38] and Hayden et al. [13] were multiplied by the area of sunscreen application in their studies (860 and 1051 cm^2, respectively) to obtain cumulative excreted BP-3.

RESULTS

Relative fugacity of BP-3 ($\acute{F}_{BP-3}$) in sunscreen products

Figure 1 shows $\acute{F}_{BP-3}$ in commercial sunscreen products, dilutions of commercial sunscreen products, and dilutions of BP-3 in Glaxal Base cream. To better visualize results, symbols represent an average of triplicate samples and are plotted on a log-log graph (See SI, Figs. S6– S8 for logarithmic graph with all sample results and linear graphs). The solid black line is the predicted $\acute{F}_{BP-3}$ based on Raoults' law assuming a homogeneous mixture of an oily medium (petrolatum or trimethylbenzen[e]indole, 35% w/w) with three active ingredients of BP-3, OMC, and 4MBC (equal %w/w of each). Moving from right to left on the black solid line, the concentration (%w/w) of the active ingredients decrease and the concentration of the inactive cream ingredients increase. In the calculation of Raoults' $\acute{F}_{BP-3}$ of BP-3, we assumed that the active ingredients do not partition into the water phase of the cream.

For the two formulations of BP-3 in Glaxal, the relationship between $\acute{F}_{BP-3}$ and %w/w is non-linear and appear to saturate at ~0.4 similar to the saturation observed for phthalates and a paraben in Glaxal in our previous study (Eftekhari et al. [40]). Therefore, as the BP-3 concentration increases in the lotion above this saturation point, we would expect dermal flux to also "saturate" and be insensitive to the concentration. This has been observed by Bunge et al. [61] for butoxyethanol absorption in rat skin from water, with a saturation occurring above ~20% butoxyethanol. They confirmed that the activity, which is analogous to fugacity in our study, of butoxyethanol flattens out above 20% butoxyethanol. However, above 80% butoxyethanol, the water content in the vehicle is small which reduces the water content of skin thereby altering the partitioning between solution and skin. Under these conditions, the model would have to account for any vehicle induced changes in the partition coefficients of skin layers.

The relative fugacities for Glaxal are substantially higher than for commercial products at the same BP-3 concentration, possibly because the composition of non-active ingredients in commercial products differs substantially from those in Glaxal (see Table S1). For the dilutions of commercial sunscreen products, the $\acute{F}_{BP-3}$ appears to be (approximately) linearly related to BP-3 mass fraction over the range tested. However, this linear relationship does not hold for $\acute{F}_{BP-3}$ vs %w/w for all individual brands of commercial sunscreen products. In other words, the $\acute{F}_{BP-3}$ of BP-3 depends on not only %w/w of BP-3 but also the sunscreen product formulation. The measured $\acute{F}_{BP-3}$ for all the commercial sunscreen products, dilutions of commercial sunscreens and two formulations of BP-3 in Glaxal are greater than the $\acute{F}_{BP-3}$ predicted by Raoults' law. This deviation of the measured $\acute{F}_{BP-3}$ from Raoult's values is anticipated because Raoult's law is applicable for dilute and ideal solutions.

The behavior of non-ideal mixtures with high concentrations of active chemicals can be difficult to predict which further emphasizes the value of directly measuring fugacities for exposure assessments. Table S2 presents measured volatile and non-volatile contents (VC and NVC) of Glaxal Base cream, Glaxal mixtures and commercial sunscreen products. The % NVC ranges from 20 to 54% in lotions, but the body stick (Neutrogena, 3% BP-3) is almost entirely non-volatile (98%). Based on the hypothesis that BP-3 partitions primarily into the NVC of the lotion, the $\acute{F}_{BP-3}$ of BP-3 is plotted as a function of its mass fraction in the whole lotion and separately in the NVC of commercial sunscreen products (Fig. 2). Figure 2 shows that the relationship between the $\acute{F}_{BP-3}$ of BP-3 and mass fraction of BP-3 in NVC of the sunscreen product roughly follows Raoult's law predictions; results plotted against the mass fraction in the whole lotion all lie above that line. Not shown in Fig. 2 are relative fugacity results from the Glaxal mixture which are much higher than results from commercial products (see Fig. 1). Combined, these observations are consistent with Glaxal having a very different base composition (mostly petrolatum, cetearyl alcohol) than commercial products, which among themselves tend to have very similar ingredients (mixed alcohols, fatty acids, fatty-acid esters, glycols, etc.). Not surprisingly, the chemical composition is as important as the NVC fraction of the product.

Results from the experiments of skin headspace SPME sampling are shown in Fig. 3. There was no significant difference between $\acute{F}_{BP-3}$ of BP-3 in lotion freshly applied to skin and the $\acute{F}_{BP-3}$ after lotion had stayed on skin for about two and half hours. For one of the sunscreen products, Hawaiian with 4% BP-3, we tried a longer skin headspace sampling of about 7 h and the $\acute{F}_{BP-3}$ was actually somewhat higher at the end than at the beginning of the experiment.

Simulation results

Figure 4 compares the experimental cumulative excreted mass of BP-3 (mg) and simulated excreted mass using base-case model parameters and varying K_{sc}. Human subjects' excretions are shown in gray. The base-case simulation is shown as a solid blue line, while simulations based on varying K_{sc} are shown in blue using two different line styles. The results of simulations based on varying other model parameters such as $\acute{F}_{BP-3}$, f_{tox}, D_{sc}, and L_{sc} for each human subject experiment can be found in the SI, Figs. S9– S12.

The predicted cumulative excreted mass using base-case parameters is below the curve and standard deviation of Gonzalez et al. [39] but higher than the cumulative BP-3 excreted by three subjects of Sarveiya et al. [38]. The base-case simulated cumulative excreted mass is well within the range of cumulative BP-3 excreted by subjects of Gonzalez et al. [15]. The total BP-3 excreted in the urine of the subjects at the end of monitoring period (48 h) are very close to the predicted mass using base-case model parameters. However, unlike predicted excretion, the cumulative excreted curve of subjects does not reach steady state by the end of monitoring period. The total reported mass excreted by the subjects in Hayden et al. experiment is very different from the three other studies, even after considering differences in the experimental approaches. We do not believe this is due to the greater total mass BP-3 of lotion applied per unit area (see Table 1). Given the magnitude of the difference (100–1000× different), we hypothesize that Hayden et al. might have either miscalculated excretion rates or misreported their units of cumulative excreted mass; the actual unit might have been µg/m^2. Also, as a minor consideration, Hayden et al. reported that 1–2% of BP-3 applied (13 g of sunscreen contained 6% BP-3 = 780 mg BP-3) was absorbed by participants. If we extract the minimum, mid, and maximum total BP-3 excreted by the

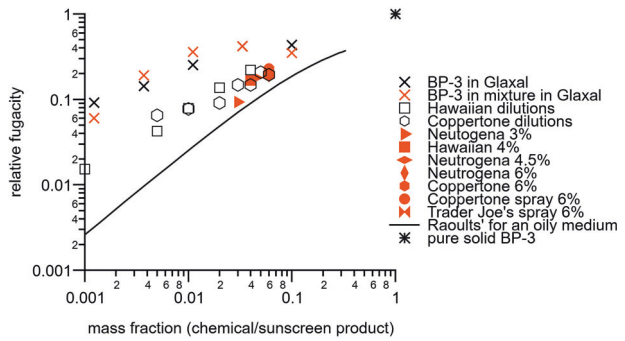

Fig. 1 Measured $\acute{F}_{BP-3}$ vs. mass fraction of BP-3 in commercial sunscreen products, dilutions of commercial sunscreen products, and mixture of BP-3 in Glaxal Base cream. The solid black line shows the $\acute{F}_{BP-3}$ prediction based on Raoults' law of BP-3 in a homogenous lipophilic fraction of the sunscreen product. All BP-3 results shown have been adjusted to account for use of solid BP-3 as the fugacity reference.

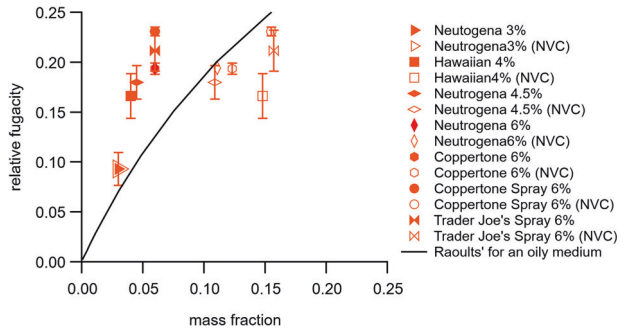

Fig. 2 Measured relative fugacity ($\acute{F}_{BP-3}$) of each commercial sunscreen product vs. BP-3 mass fraction (total sunscreen and in non-volatile content (NVC)) of the sunscreen product. Average of three to four headspace SPME analysis and error bar indicating their standard deviations are shown in the graph.

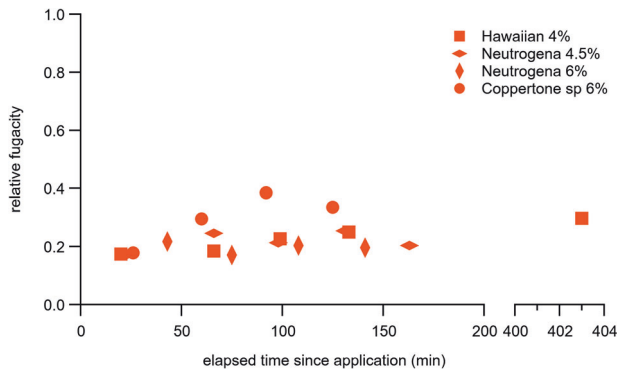

Fig. 3 Relative fugacity ($\acute{F}_{BP-3}$) of BP-3 of commercial sunscreen on human skin vs elapsed time (time since sunscreen was applied on skin).

subjects reported in Hayden et al., we obtain 0.7, 3.4, and 5.4% absorbed which is a bit higher than the range of 1–2%. To absorb that fraction of BP-3 from such a thick layer of lotion is unlikely and would be the result of a (possibly) unrealistic permeability.

Varying individual parameters (SI, Figs. S9–S12) results in simulations that approach or cross into the lower standard deviation of human subject data. In general, however, simulations, even when varying parameters (one at a time) within reasonable ranges, tend to under predict the results of Gonzalez et al. [39]. Model predictions are, as expected, proportional to the choice of $\acute{F}_{BP-3}$ and the f_{tox}. A smaller L_{sc} results in a larger cumulative excreted mass which also occurs earlier compared with a larger L_{sc}. Higher values of both D_{sc} and K_{sc} result in cumulative excreted mass in the range of cumulative mass of BP-3 excreted from human subject experiment. For Gonzalez et al. [39] all simulations reach a plateau around 120 h after the beginning of experiment; while the flattening of subjects' data does not happen until 150 h after the beginning of experiment. Unlike simulation of Gonzalez et al. [39] the predicted results using base-case model input parameters are higher than the cumulative BP-3 excreted by three subjects of Sarveiya et al. [38]. However, lower values of most of the variables predict excreted mass very close to that of the Sarveiya et al. subjects [38]. Larger D_{sc} and smaller L_{sc} not only increase the steady state excreted mass of BP-3; but also increase the slope of curve which results in a much faster increase in BP-3 urinary excretion which is inconsistent with the gradual increase observed in Sarveiya et al. [38].

For Gonzalez et al. [15] the total BP-3 excreted in the urine of the subjects at the end of monitoring period (48 h) are very close to the predicted mass using base-case model parameters. However, unlike predicted excretion, the cumulative excretion curve of subjects does not reach steady state by the end of monitoring period. Both lower and higher values of $\acute{F}_{BP-3}$, f_{tox}, and L_{sc} results in predictions in the range of the subjects' BP-3 excretion. Increasing either D_{sc} or K_{sc} by a factor of three results in approximately the same total excretion of BP-3, which is about 1.8 times larger than the total maximum BP-3 excreted by subjects. But the increase in cumulative excreted BP-3 is more gradual using three K_{sc} than three D_{sc}. Decreasing D_{sc} by a factor of 3 reduces cumulative excretion but also delays the flattening of the cumulative excretion curve by ~15 h relative to the base case simulation.

For Hayden et al. [13] the total excreted mass of BP-3 predicted by the model is about 17, 67, and 107 times lower than the min, mid, and max mass excreted by the subjects. The base case simulation predicts about 0.5 mg of BP-3 excreted, which is very similar to the predictions and experimental excreted mass of Sarveiya et al. [38]. Despite very similar experimental parameters, such as area and time applied, Hayden et al. reported about 815 times higher BP-3 excreted mass than Sarveiya et al., considering average excreted mass for both human subject experiments. One notable methodological difference between the studies was that Hayden et al. applied a lotion thickness that was six times greater than any other human subject experiment including Sarveiya et al. Since the thickness of lotion does not affect initial fugacity of BP-3 from a sunscreen product (which is the actual driving force for transdermal uptake of BP-3 from sunscreen product), and only a small fraction of BP-3 is absorbed from even the thinnest coating applied among studies, the excreted BP-3 mass from subjects of Hayden et al. and Sarveiya et al. are expected to be much closer to each other than the reported values.

DISCUSSION

In Fig. 5a, the predicted and experimental excreted mass of BP-3 for all human subject experiments are presented. The low and high ends of the model bars represent the minimum and maximum excretion of the sensitivity test. The model predictions are reasonably consistent with the results of Sarveiya et al. [38] and Gonzalez et al. [15]. However, there is no overlap between predicted and experimental excreted mass for Hayden et al. [13] and Gonzalez et al. [39]. The model predicts lower range of excreted mass for both Gonzalez et al. [39] and Hayden et al. [13]. Many factors can influence the results of such studies and they are not expected to align perfectly. Key factors that separate these studies are the area of skin covered with sunscreen, the total time the sunscreen product stayed on the skin of subjects

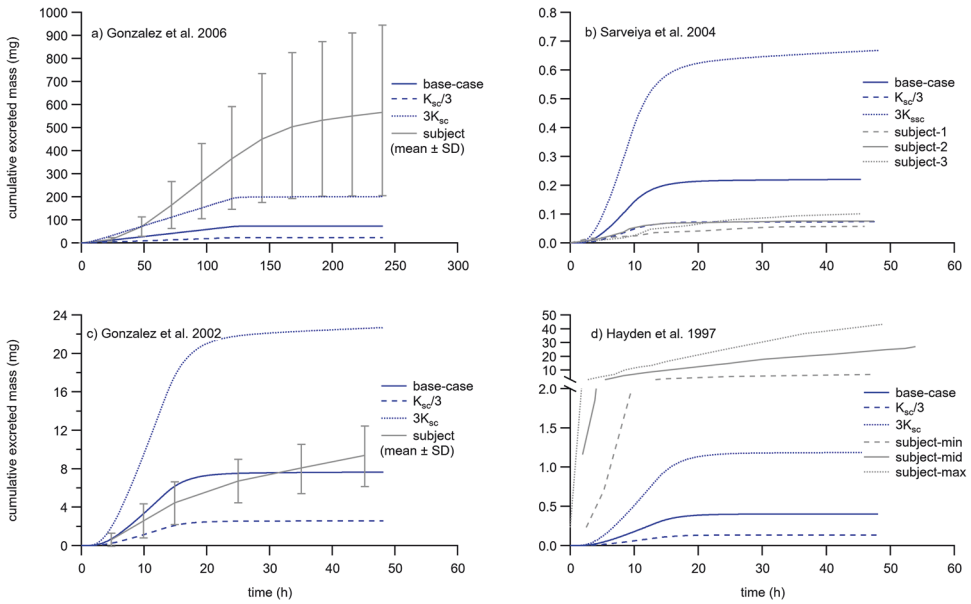

Fig. 4 Experimental (Gonzalez et al. [39] Sarveiya et al. [38] Gonzalez et al. [15], and Hayden et al. [13]) and simulated cumulative excreted mass of BP-3 (mg) vs time (h). The mean of experimental cumulative mass is shown in gray with error bars indicate standard deviations (SD). The base-case simulation is shown as a solid blue line, while simulations based on varying K_{sc} are shown in blue using two different line styles. The results of simulations based on varying other model parameters such as relative fugacity ($\acute{F}_{BP-3}$) toxicokinetic factor (f_{tox}), diffusion to stratum corneum (D_{sc}), and stratum corneum thickness (L_{sc}) for each human subject experiment can be found in the SI, Figs. S9–S12.

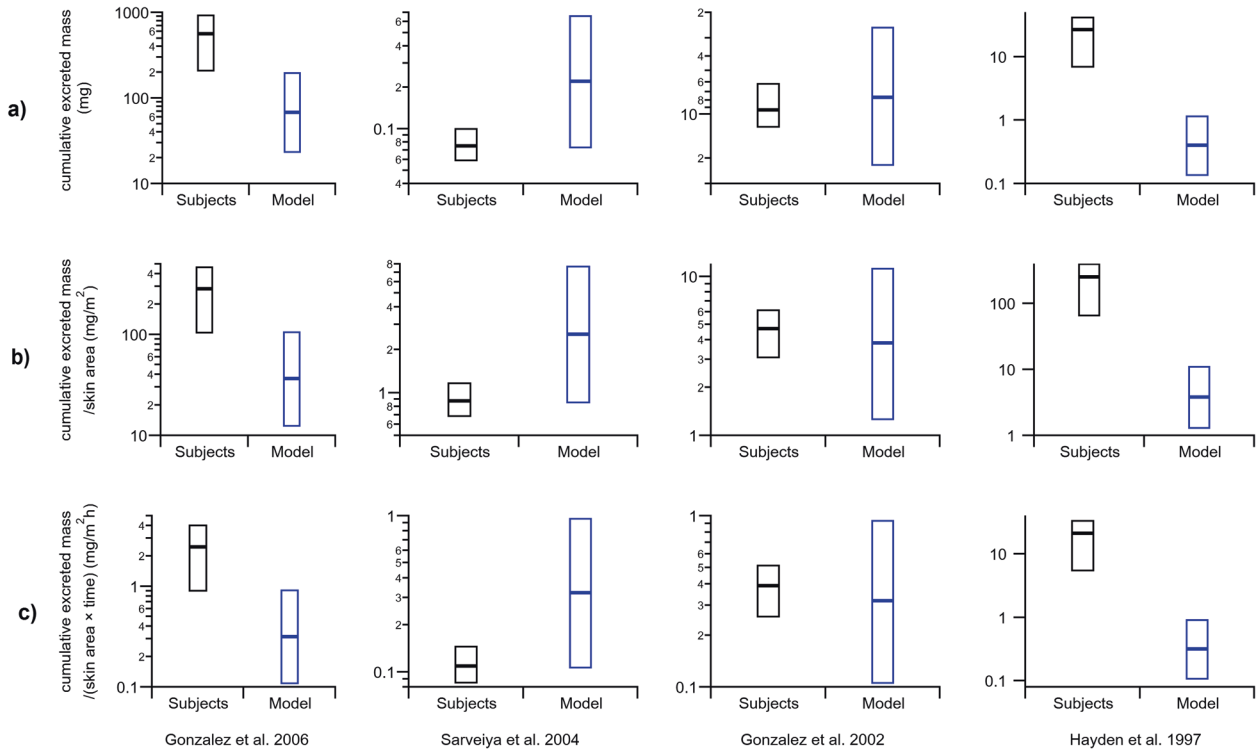

Fig. 5 Experimental vs. simulated total excreted mass of BP-3 for all human subject scenarios. a Total excreted mass of BP-3 by subjects of each human subject experiment vs. estimated BP-3 excreted. **b** Total excreted mass of BP-3 (mg) normalized by skin area of lotion application (m^2) by subjects of each human subject experiment vs. estimated BP-3 excreted. **c** Total excreted mass of BP-3 (mg) normalized by skin area of lotion application (m^2) and time that lotion stayed on skin (h) by subjects of each human subject experiment vs. estimated BP-3 excreted. Subjects' box shows minimum, mid or average (depends on available data from human subject experiments), and maximum. Model's box shows minimum estimated excreted mass obtained by varying variables, base-case estimated mass, and maximum estimated cumulative excreted mass obtained by varying variables.

(inclusive of multiple applications), and any differences among lotion formulations.

To better compare the results of human subjects, excreted BP-3 mass was normalized first by skin area of sunscreen application (Fig. 5b) and then by both area and the total time the sunscreen stayed on skin in each experiment (Fig. 5c). Fundamentally, area covered should be linearly related to the total mass absorbed or excreted (assuming all skin regions have the same permeability [62, 63]). Although time is not a linear parameter in transdermal uptake, this can roughly normalize the data from human subject experiments with different experimental conditions.

In Fig. 5c, the first three studies (left to right) are similar in magnitude, although ranging from 0.15 to 2.5 mg/m^2/h. Our simulation results lie in the middle of this range (~0.3 mg/m^2/h), providing support for the basic approach. Still, there are enough differences among the three human subject experiments that we should consider other influential variables. Certainly, there are differences among the subject population that could influence outcomes. For example, Sarveiya et al. [38] included three female subjects, and only tested a relatively small area of the forearms and back. On the other hand, the two Gonzalez studies both used larger study populations (10–11 mixed sex subjects for Gonzalez et al. [15] and 25 mixed sex subjects for Gonzales et al. [39]), the same whole-body coverage and both used a 4% BP-3 lotion. Despite these similarities, the mean flux (Fig. 5c) is 0.38 mg/m^2/h in the 2002 study and 2.5 mg/m^2/h in the 2006 study, which is a large difference for two populations treated, presumably, identically.

Another possibility is that the lotion formulations were different enough to result in major differences in transdermal permeation. We show that modern sunscreens (Figs. 1and 3) have fugacities for 3–6% BP-3 sunscreen lotions that lie within a relatively narrow range (0.15–0.23 $\acute{F}_{BP-3}$). However, the in-house mixture in Glaxal had a relative fugacity of BP-3 that was about three times higher than for commercial sunscreens with similar BP-3 content. Also, Neutrogena body stick had a lower $\acute{F}_{BP-3}$ of 0.09, which is likely due to the high mass fraction of organic/oily components in the mixture (Fig. 2). Therefore, it is possible that Gonzalez et al. [39] used a formulation with a low organic content (which increases fugacity) and Gonzalez et al. [15] used a formulation with a higher organic content. The true fugacity of the lotion used in these human subject studies remains an important unknown. These normalizations further suggest that Hayden et al. [13] might have misreported the data or the units. The normalized values (Fig. 5c) from Hayden et al. are ten times greater than the highest reported by Gonzalez et al. [39].

In conclusion, the mechanistic model combined with measured fugacity generated predictions that were within a factor of three of two of the four human subject experiments available in the literature. The model underpredicted excreted mass for two of the studies, but this could be due to limitations on the quality of input variable values (e.g., BP-3 fugacity in lotions used in those studies) or possibly data reporting errors. In our previous studies (Eftekhari et al. [40]), we concluded that measured fugacity in combination with our model provided order-of-magnitude accurate predictions of transdermal uptake of two phthalates and a paraben from lotion (Eftekhari et al. [40]) as well as BP-3 uptake from clothing (Eftekhari et al. [49]). Considering these studies together, we believe that the measured fugacity is an important element of exposure assessment and would be particularly valuable when combined with in vivo studies of transdermal uptake of chemicals from a wide variety of sources including consumer products, soil, water, textiles, toys and building surfaces.

REFERENCES

1. Pathak MA. Sunscreens: topical and systemic approaches for protection of human skin against harmful effects of solar radiation. J Am Acad Dermatol. 1982. https://doi.org/10.1016/S0190-9622(82)70117-3.
2. Pathak MA. Sunscreens: topical and systemic approaches for the prevention of acute and chronic sun-induced skin reactions. Dermatol Clin. 1986;4:321–34.
3. Nash JF. Human safety and efficacy of ultraviolet filters and sunscreen products. Dermatol Clin. 2006;24:35–51.
4. Lautenschlager S, Wulf HC, Pittelkow MR. Photoprotection. Lancet. 2007;370:528–37.
5. Jansen R, Wang SQ, Burnett M, Osterwalder U, Lim HW. Photoprotection: Part I Photoprotection by naturally occurring, physical, and systemic agents. J Am Acad Dermatol. 2013;69:853.e1–853.e12.
6. Krause M, Klit A, Blomberg Jensen M, Søeborg T, Frederiksen H, Schlumpf M, et al. Sunscreens: are they beneficial for health? An overview of endocrine disrupting properties of UV-filters. Int J Androl. 2012;35:424–36.
7. Thompson SC, Jolley D, Marks R. Reduction of solar keratoses by regular sunscreen use. N Engl J Med. 1993;329:1147–51.
8. Green A, Williams G, Neale R, Hart V, Leslie D, Parsons P, et al. Daily sunscreen application and betacarotene supplementation in prevention of basal-cell and squamous-cell carcinomas of the skin: a randomised controlled trial. Lancet. 1999;354:723–9.
9. Dupuy A, Dunant A, Grob JJ. Randomized controlled trial testing the impact of high-protection sunscreens on sun-exposure behavior. Arch Dermatol. 2005;141:950–6.
10. Hagedorn-Leweke U, Lippold BC. bsorption of sunscreens and other compounds through human skin in vivo: derivation of a method to predict maximum fluxes. Pharm Res J Am Assoc Pharm Sci. 1995;12:1354–60.
11. Treffel P, Gabard B. Skin penetration and sun protection factor of ultra-violet filters from two vehicles. Pharm Res. 1996;13:770–4.
12. Walters KA, Brain KR, Dressler WE, Green DM, Howes D, James VJ, et al. Percutaneous penetration of N-nitroso-N-methyldodecylamine through human skin in vitro: application from cosmetic vehicles. Food Chem Toxicol. 1997;35:705–12.
13. Hayden CGJ, Roberts MS, Benson HAE. Systemic absorption of sunscreen after topical application. Lancet. 1997;350:863–4.
14. Jiang R, Roberts MS, Collins DM, Benson HAE. Absorption of sunscreens across human skin: an evaluation of commercial products for children and adults. Br J Clin Pharm. 1999;48:635–7.
15. Gonzalez H, Farbrot A, Larkö O. Percutaneous absorption of benzophenone-3, a common component of topical sunscreens. Clin Exp Dermatol. 2002;27:691–4.
16. Janjua NR, Mogensen B, Andersson AM, Petersen JH, Henriksen M, Skakkebæk NE, et al. Systemic absorption of the sunscreens benzophenone-3, octyl- methoxycinnamate, and 3-(4-methyl-benzylidene) camphor after whole-body topical application and reproductive hormone levels in humans. J Invest Dermatol. 2004;123:57–61.
17. Kaidbey K, William Gange R. Comparison of methods for assessing photoprotection against ultraviolet A in vivo. J Am Acad Dermatol. 1987;16:346–53.
18. Schlumpf M, Cotton B, Conscience M, Haller V, Steinmann B, Lichtensteiger W. In vitro and in vivo estrogenicity of UV screens. Environ Health Perspect. 2001. https://doi.org/10.1289/ehp.01109239.
19. Schreurs R, Lanser P, Seinen W, Van der Burg B. Estrogenic activity of UV filters determined by an in vitro reporter gene assay and an in vivo transgenic zebrafish assay. Arch Toxicol. 2002;76:257–61.
20. Ma R, Cotton B, Lichtensteiger W, Schlumpf MUV. filters with antagonistic action at androgen receptors in the MDA-kb2 cell transcriptional-activation assay. Toxicol Sci. 2003;74:43–50.
21. Witorsch RJ, Thomas JA. Personal care products and endocrine disruption: a critical review of the literature. Crit Rev Toxicol. 2010;40:1–30.
22. Wang SQ, Burnett ME, Lim HW. Safety of oxybenzone: putting numbers into perspective. Arch Dermatol. 2011;147:865–6.
23. Chen M, Tang R, Fu G, Xu B, Zhu P, Qiao S, et al. Association of exposure to phenols and idiopathic male infertility. J Hazard Mater. 2013;250–251:115–21.
24. Tang R, Chen MJ, Ding GD, Chen XJ, Han XM, Zhou K, et al. Associations of prenatal exposure to phenols with birth outcomes. Environ Pollut. 2013;178:115–20.
25. Ghazipura M, McGowan R, Arslan A, Hossain T. Exposure to benzophenone-3 and reproductive toxicity: a systematic review of human and animal studies. Reprod Toxicol. 2017;73:175–83.
26. Kadry AM, Okereke CS, Abdel-Rahman MS, Friedman MA, Davis RA. Pharmacokinetics of benzophenone-3 after oral exposure in male rats. J Appl Toxicol. 1995;15:97–102.
27. Okereke CS, Kadry AM, Abdel-Rahman MS, Davis RA, Friedman MA. Metabolism of benzophenone-3 in rats. Drug Metab Dispos. 1993:21;788--91.
28. Wang L, Kannan K. Characteristic profiles of benzonphenone-3 and its derivatives in urine of children and adults from the United States and China. Environ Sci Technol. 2013;47:12532–8.
29. Suzuki T, Kitamura S, Khota R, Sugihara K, Fujimoto N, Ohta S. Estrogenic and antiandrogenic activities of 17 benzophenone derivatives used as UV stabilizers and sunscreens. Toxicol Appl Pharm. 2005;203:9–17.
30. Kunisue T, Chen Z, Buck Louis GM, Sundaram R, Hediger ML, Sun L, et al. Urinary concentrations of benzophenone-type UV filters in U.S. women and their association with endometriosis. Environ Sci Technol. 2012;46:4624–32.

31. Wolff MS, Engel SM, Berkowitz GS, Ye X, Silva MJ, Zhu C, et al. Prenatal phenol and phthalate exposures and birth outcomes. Environ Health Perspect. 2008; 116:1092–7.
32. Philippat C, Mortamais M, Chevrier C, Petit C, Calafat AM, Ye X, et al. Exposure to phthalates and phenols during pregnancy and offspring size at birth. Environ Health Perspect. 2012;120:464–70.
33. Ferguson KK, Meeker JD, Cantonwine DE, Mukherjee B, Pace GG, Weller D, et al. Environmental phenol associations with ultrasound and delivery measures of fetal growth. Environ Int. 2018;112:243–50.
34. Food and Drug Administration H. Labeling and effectiveness testing; sunscreen drug products for over-the-counter human use. Final rule Fed Regist 2011;76:35620–65.
35. Xue J, Liu W, Kannan K. Bisphenols, benzophenones, and bisphenol A diglycidyl ethers in textiles and infant clothing. Environ Sci Technol. 2017;51:5279–86.
36. Li AJ, Kannan K. Elevated concentrations of bisphenols, benzophenones, and antimicrobials in pantyhose collected from six countries. Environ Sci Technol. 2018;52:10812–9.
37. European Commission. Scientific Committee on Consumer Products Benzophenone-3. 2008.
38. Sarveiya V, Risk S, Benson HAE. Liquid chromatographic assay for common sunscreen agents: application to in vivo assessment of skin penetration and systemic absorption in human volunteers. J Chromatogr B Anal Technol Biomed Life Sci. 2004;803:225–31.
39. Gonzalez H, Farbrot A, Larkö O, Wennberg AM. Percutaneous absorption of the sunscreen benzophenone-3 after repeated whole-body applications, with and without ultraviolet irradiation. Br J Dermatol. 2006;154:337–40.
40. Eftekhari A, Frederiksen H, Andersson AM, Weschler CJ, Weschler CJ, Morrison G. Predicting transdermal uptake of phthalates and a paraben from cosmetic cream using the measured fugacity. Environ Sci Technol. 2020;54:7471–84.
41. Mackay D. Finding fugacity feasible. Environ Sci Technol. 1979;13:1218–23.
42. MacKay D, Arnot JA. The application of fugacity and activity to simulating the environmental fate of organic contaminants. J Chem Eng Data. 2011;56:1348–55.
43. Golding CJ, Gobas FAPC, Birch GF. A fugacity approach for assessing the bioaccumulation of hydrophobic organic compounds from estuarine sediment. Environ Toxicol Chem. 2008;27:1047–54.
44. Mackay D, Paterson S. Fugacity revisited: the fugacity approach to environmental transport. Environ Sci Technol. 1982;16:654A–660A.
45. Schramm KW. Environmental impact assessment (EIA): equilibrium fugacity calculations and worst case approach. Chemosphere. 1994;28:2151–71.
46. Mackay D, Paterson S. Fugacity approach for calculating near-source toxic substance concentrations and partitioning in lakes. Water Pollut Res J Can. 1981;16:59–70.
47. Lago AF, Jimenez P, Herrero R, Dávalos JZ, Abboud JLM. Thermochemistry and gas-phase ion energetics of 2-hydroxy-4-methoxy- benzophenone (oxybenzone). J Phys Chem A. 2008;112:3201–8.
48. Duffy E, Jacobs MR, Kirby B, Morrin A. Probing skin physiology through the volatile footprint: Discriminating volatile emissions before and after acute barrier disruption. Exp Dermatol. 2017;26:919–25.
49. Eftekhari A, Hill JT, Morrison GC. Transdermal uptake of benzophenone-3 from clothing: comparison of human participant results to model predictions. J Expo Sci Environ Epidemiol. 2020;31:149–57.
50. Okereke CS, Abdel-Rhaman MS, Friedman MA. Disposition of benzophenone-3 after dermal administration in male rats. Toxicol Lett. 1994;73:113–22.
51. Wang TF, Kasting GB, Nitsche JM. A multiphase microscopic diffusion model for stratum corneum permeability. I. Formulation, solution, and illustrative results for representative compounds. J Pharm Sci. 2006;95:620–48.
52. Wang TF, Kasting GB, Nitsche JM. A multiphase microscopic diffusion model for stratum corneum permeability. II. Estimation of physicochemical parameters, and application to a large permeability database. J Pharm Sci. 2007;96:3024–51.
53. Weschler CJ, Nazaroff WW. Semivolatile organic compounds in indoor environments. Atmos Environ. 2008;42:9018–40.
54. Gong M, Zhang Y, Weschler CJ. Predicting dermal absorption of gas-phase chemicals: transient model development, evaluation, and application. Indoor Air. 2014;24:292–306.
55. Morrison GC, Weschler CJ, Bekö G. Dermal uptake directly from air under transient conditions: advances in modeling and comparisons with experimental results for human subjects. Indoor Air. 2016;26:913–24.
56. Egawa M, Hirao T, Takahashi M. In vivo estimation of stratum corneum thickness from water concentration profiles obtained with raman spectroscopy. Acta Derm Venereol. 2007;87:4–8.
57. Rushmer RF, Buettner KJK, Short JM, Odland GF. The skin. Science. 1966;154:343–8.
58. Cleek RL, Bunge AL. A new method for estimating dermal absorption from chemical exposure. 1. General approach. Pharm Res J Am Assoc Pharm Sci. 1993;10:497–506.
59. Morrison GC, Weschler CJ, Bekö G. Dermal uptake of phthalates from clothing: comparison of model to human participant results. Indoor Air. 2017;27:642–9.
60. Weschler CJ, Nazaroff WW. SVOC exposure indoors: fresh look at dermal pathways. Indoor Air. 2012;22:356–77.
61. Bunge AL, Persichetti JM, Payan JP. Explaining skin permeation of 2-butoxyethanol from neat and aqueous solutions. Int J Pharm. 2012;435:50–62.
62. Holbrook KA, Odland GF. Regional differences in the thickness (cell layers) of the human stratum corneum: an ultrastructural analysis. J Invest Dermatol. 1974;62: 415–22.
63. Yosipovitch G, Maayan-Metzger A, Merlob P, Sirota L. Skin barrier properties in different body areas in neonates. J Am Acad Pediatr. 2000. https://doi.org/10.1542/peds.106.1.105.

ACKNOWLEDGEMENTS

The authors would like to thank the Center for Research in Energy and the Environment (CREE) of the Missouri University of Science & Technology for their help with the instruments. The modeling component of this research was supported by the Alfred P. Sloan Foundation through the Modelling Consortium for Chemistry of Indoor Environments (MOCCIE 1, G-2017–9796 and MOCCIE 2, G-2019-12306).

AUTHOR CONTRIBUTIONS

AE collected data, generated model simulations, drafter and revised the manuscript. GCM conceived of the work, supervised model simulations, revised the manuscript. All authors approved of the final version and agreed to be accountable for all aspects of the work.

COMPETING INTERESTS

The authors declare no competing interests.

ADDITIONAL INFORMATION

Supplementary information The online version contains supplementary material available at https://doi.org/10.1038/s41370-021-00383-9.

Correspondence and requests for materials should be addressed to Azin Eftekhari.

Reprints and permission information is available at http://www.nature.com/reprints

Publisher's note Springer Nature remains neutral with regard to jurisdictional claims in published maps and institutional affiliations.